Humanoid Robot Balance Control Using CoM Height Variations

B.J. van Hofslot

Master of Science Thesis

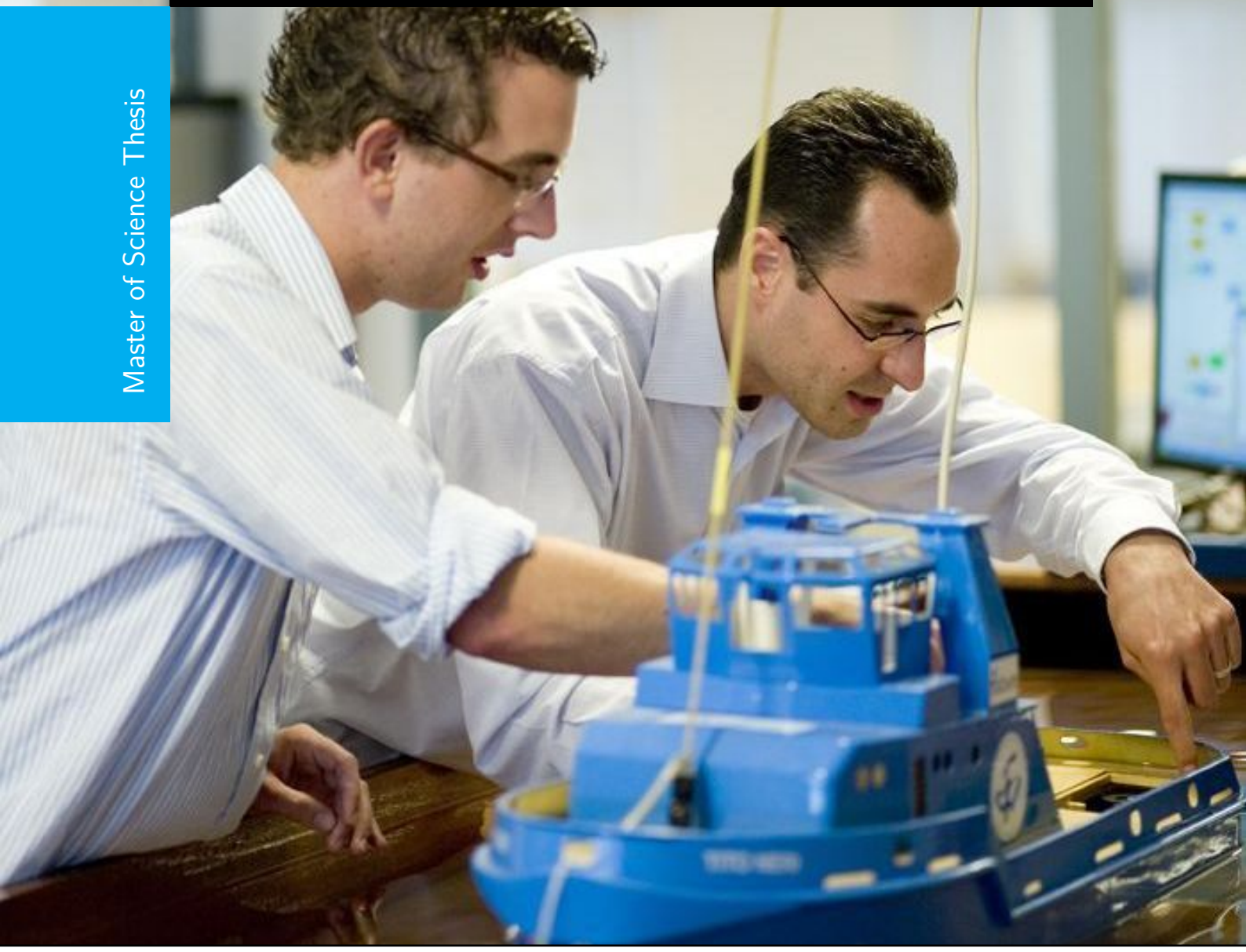

TU Delft Delft University of Technology

Cognitive Robotics

Humanoid Robot Balance Control Using CoM Height Variations

Master of Science Thesis

For the degree of Master of Science in Systems and Control at Delft University of Technology

B.J. van Hofslot

October 8, 2018

Faculty of Mechanical, Maritime and Materials Engineering (3mE) · Delft University of Technology

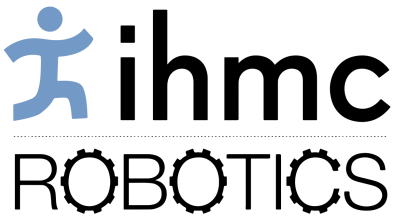

The work in this thesis was supported by the Institute for Human and Machine Cognition. Their cooperation is hereby gratefully acknowledged.

Abstract

This is an abstract.

Table of Contents

List of Figures

List of Tables

Preface

According to WikipediA, a preface (pronounced "*preffus*") is an introduction to a book written by the author of the book. In this preface I can discuss the interesting story of how this thesis came into being.

This is document is a part of my Master of Science graduation thesis. The idea of doing my thesis on this subject came after a discussion with my good friends Tweedledum and Tweedledee...

Acknowledgements

I would like to thank my supervisor prof.dr.ir. M.Y. First Reader for his assistance during the writing of this thesis...

By the way, it might make sense to combine the Preface and the Acknowledgements. This is just a matter of taste, of course.

Delft, University of Technology
October 8, 2018

B.J. van Hofslot

"Playing football is very simple, but playing simple football is the hardest thing there is."

— *Johan Cruyff*

Chapter 1

Introduction

1-1 Motivation

Distinguish different goals of publication: [1]

- Improve behavior over rough-terrain
- Minimize energy consumption or mimic natural behavior
- Analyse the effects of height variation
- Extend control authority by using height variations

1-2 Research Objective

In this thesis is focussed on the last two goals. Exploring the effects of height variation. Extend the control authority by using height variations

1-3 Contributions

- Theoretic Limits on Capture
- Orbital Energy MPC
- Approaches for application on real robot

1-4 Thesis Outline

Chapter 2

Background

2-1 Modeling of Walking

2-1-1 Simple Walking Model

Mass, inertia, finite-sized foot.

2-1-2 Linear Inverted Pendulum Model

In modeling of walking, one of the most important assumptions often made is the modeling of the stance leg as a linear inverted pendulum (LIP), as for example in [2]. Besides this, a not-linearized inverted pendulum is also widely used in the modeling of walking [3]. For planning and control however, a linearized description is desirable. In the two-dimensional space (2D) LIP equations of motion

$$\ddot{x} = \frac{g}{l}x \tag{2-1}$$

where l is the pendulum length and x the Cartesian x-coordinate of the pendulum tip, the motion of the tip along the x-axis does not affect l. At any position x, a local virtual straight pendulum can be considered, so this motion is at a constant height and $l = z_0$ holds. As in three-dimensional space (3D) by the linear model the system dynamics can be decoupled, the dynamics in y-direction read the same: $\ddot{y} = \frac{g}{l}y$. In Figure 2-1 this motion is visualized if the center of mass (CoM) is relatively far from from the base. The pendulum base lies in the origin and $\boldsymbol{x} = [x, y]^T$ is the 2D CoM projection on the horizontal plane. Because the LIP assumption holds, the vertical component of the leg force $\boldsymbol{f}$ has to cancel out gravity acceleration: $f_z = mg$.

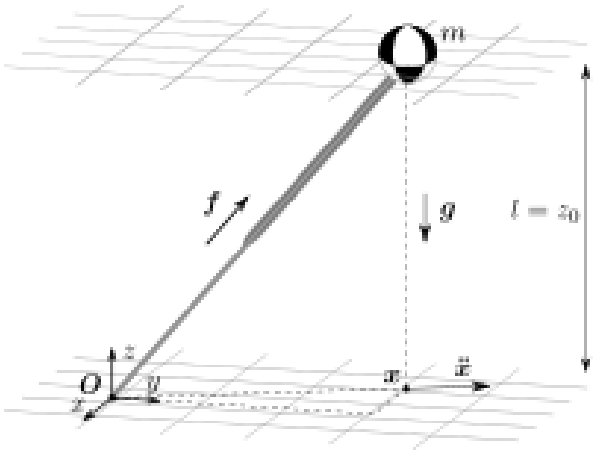

Figure 2-1: 3D motion of LIP model.

2-1-3 Nonlinear Models

2-2 Measured Quantities & Ground Reference Points in Walking

2-2-1 Ground Reaction Force

A common approach for quantifying the dynamics of a walker, either a human or a robot, is the use of a ground reaction force (GRF), coming a from a single point of application on the ground. The magnitude and direction of the force vector, the gravitational vector, other external forces and the robots state determine the dynamics of the system.

2-2-2 The center of pressure (CoP)

The feet attached to the LIP robot model increase the possibilities to control its motion. The ankles can apply a torque that would virtually move the position of the base of the inverted pendulum, so that the linear acceleration on the CoM as in Eq. (2-1) and the capture point as in Eq. (2-7) change. The new virtual base is called the CoP. By its definition, this point only lives within the support polygon [4]. In Figure 2-2 the definition of the CoP is visualized. If the point mass is restricted to move on a constant height, the vertical component of $\boldsymbol{f'}$ counteracts gravity: $f'_z = g$.

2-2-3 The zero moment point (ZMP)

The ZMP coincides during stable walking with the CoP, like described in [4]. The two points however are not equal in unstable or more complicated cases, like falling over. The CoP is restricted to be in the support polygon, as this is a point that links to contact forces [5]. The ZMP however is not restricted to lie within the support polygon. The ZMP is the point on the ground where the tipping moment equals zero. The tipping moment is defined as the component of the moment that is tangential to the ground surface. The ZMP initially was introduced in [6].

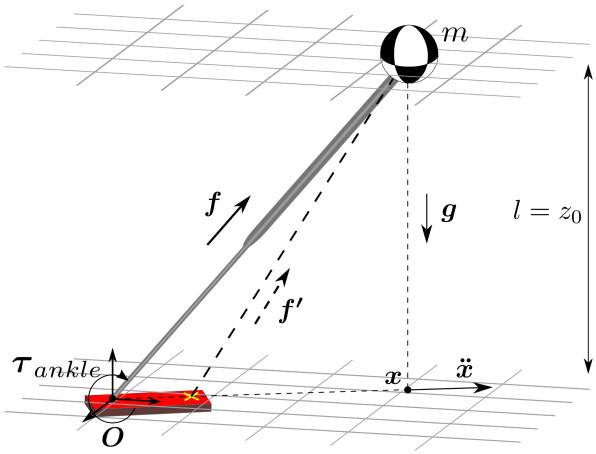

Figure 2-2: 3D motion of LIP model with foot. The yellow cross points out the CoP location.

2-2-4 The centroidal momentum pivot (CMP)

The earlier mentioned points give sufficient measure for a LIP model with point mass and finite-sized feet. However, any angular momentum applied by the body does not affect those points. In the case of the CoP for example, the model assumes the resulting reaction force acts from the CoP through the CoM. The CMP takes angular momentum into account, which can be used as a measure and for control [7]. This is defined as the point where a line passing through the CoM, parallel to the ground reaction force intersects with the ground surface. The CMP is defined as

$$x_{CMP} = x_{ZMP} + \frac{\tau_{y,CoM}}{F_{gr,z}} \tag{2-2}$$

$$y_{CMP} = y_{ZMP} - \frac{\tau_{x,CoM}}{F_{gr,z}} \tag{2-3}$$

where τ_{CoM} is the torque around the CoM, $[x_{ZMP}, y_{ZMP}]$ the ZMP location on the horizontal plane and $F_{gr,z}$ is the ground reaction force in z-direction in Cartesian space. In Figure 2-3 is displayed how body angular momentum affects the ground reaction force $\boldsymbol{f'}$ from the CoP and how the CMP can be determined with the intersection of a parallel line through the CoM and the ground plane. For clarity the point in the image lies on the line from $\boldsymbol{O}$ to $\boldsymbol{x}$. This has not to be the case however, as the body can exert angular momentum along all axes.

2-2-5 Other Points

2-3 Energy of Walking

2-3-1 LIP Orbital Energy

A crucial finding in an extended use of LIP models can be found in [8]. Because force is mass times acceleration: $F = ma$, impuse momentum is force times velocity: $I = Fv$ and the energy or work done by a force is the force times the distance, and thus the impulse integrated

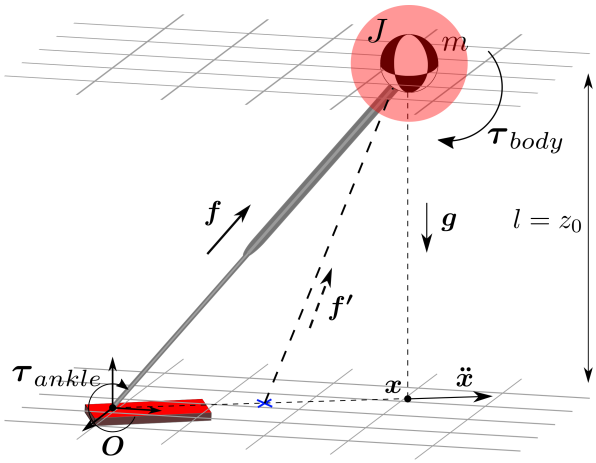

Figure 2-3: 3D motion of LIP model with foot and body inertia. The blue cross points out the CMP location.

over the time interval: $E = Fs = \int Fvdt$, there can be reasoned that if one takes the time integral of the product of the second and the first derivative of a state, an expression for a normalized energy can be achieved: $\frac{E}{m} = \int avdt$. In the mentioned publication that same action is applied on Eq. (2-1):

$$\int (\ddot{x} - \frac{g}{l}x)\dot{x}dt = \frac{1}{2}\dot{x}^2 - \frac{g}{2z_0}x + C = 0 \tag{2-4}$$

with C the integration constant. The LIP Orbital Energy is defined as $E_{LIP} = -C$. If $E_{LIP} > 0$, the point mass will cross the x position of the pendulum base with its current velocity. If $E_{LIP} < 0$, the point mass will not cross the pendulum base and will have a turning point where the velocity becomes zero.

The instantaneous capture point (ICP)

Although the finding of the LIP Orbital Energy was very important for future robot motion modeling, more than a decade later [9] introduced the capture point (CP). Taking $E_{LIP} = 0$ and taking the square root of Eq. (2-4) gives

$$x_{CP} = \sqrt{\frac{z_0}{g}}\dot{x} \tag{2-5}$$

where x_{CP} is the CP, measured from the current pendulum tip position, based on the current tip velocity $\dot{x}$. This is the point where the velocity is exactly driven to zero and the pendulum is upright, where neither crossing of the pendulum base ocurred nor turning of body velocity. In Figure 2-4 a 2D visual explanation is given of this point. Later, the ICP was introduced [10], which gives a slightly different discription of the point:

$$x_{ICP} = x + \sqrt{\frac{z_0}{g}}\dot{x} \tag{2-6}$$

where x_{ICP} is the ICP. In this way, the point can be described in the environment coordinates. The x- and y-coordinate can be decoupled as in the equations of motion of Eq. (2-1). However,

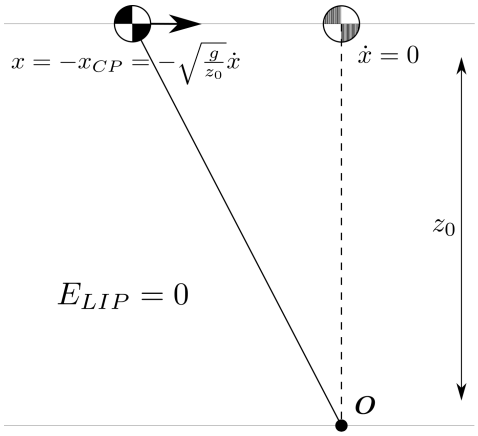

Figure 2-4: Visualization of path and states by the capture of the point mass according ICP theory.

in the 2D horizontal plane, convergence to the capture point in one direction does not include convergence to the capture point in the other. In other words: the direction of motion is not restricted to move towards the pendulum base as in the sideview case.

ICP dynamics

Because the ankle is not always located at the same location as the ICP for the current horizontal velocity, for modeling and planning the time derivative is taken of the ICP, which is named the ICP dynamics [10]. This time derivative can be written as a function of the current ICP location:

$$\dot{\boldsymbol{x}}_{ICP} = \sqrt{\frac{g}{z_0}}\boldsymbol{x}_{ICP} \tag{2-7}$$

where $\boldsymbol{x}_{ICP}$ is the xy-vector of the ICP location and assuming that the pendulum base is the origin.

2-3-2 Nonlinear Orbital Energy

E_{orbit}[11]

2-3-3 Boundedness Condition

[12]

2-4 Related Works CoM Height Variation

2-4-1 Planning & Gait Generation

[13] [14]

2-4-2 Effects of Height Variation

[3] [15] [16]

2-4-3 Control for Balance

[1] [17]

2-5 Humanoid Robotics at IHMC

2-5-1 Robots

Atlas, Valkyrie.

2-5-2 Planning

Footstep Planning

User defined. A*. Terrain information given (LiDAR).

ICP Planning

Dynamic planning. Basic approach (CoP knotpoints, integration of icp dynamics). Current improvements (double support, heel-toe, angular momentum, continous cop/cmp trajectories).

2-5-3 ICP Control

CMPd - linear momentum rate of change.

2-5-4 Momentum-based Control & Inverse Dynamics

QP inputs. Robot Joints. Trade off between different tasks. Jacobian. Accounting for robustness compared to linear plan (height variations / impact). Task-priority (null space projection/singularity avoidance).

Chapter 3

Theoretic Limits on Capture

Common approach to model robot of a mass subject to a ground reaction force coming form a single point of application. Refer to sections in background.
In this case there is looked at the point foot - point mass model, so no angular momentum is included.
This chapter matches the goal of exploring the effects of height variation.
Common habit is to formulate optimization problem, and to solve 'let the optimization figure it out', but there is not looked at limits.

3-1 Unconstrained Capture Region

INCLUDE HEIGHT VELOCITY In the point-foot, point-mass model with prismatic leg joint, the constraints are:

- Unilateral ground reaction force
- Limit on leg length
- Limit on leg force
- Limit on ground friction

In this section the bounds are given with respect to capturability of a horizontally traveling CoM, like with the study of the capture point and orbital energy cousines. The only constraint taken into account is unilaterality of GRF. Also a measure of this limit is given in terms of the CP.
Balistic touchdown time for a given height is:

$$t = \sqrt{\frac{2z_0}{g}} \tag{3-1}$$

The horizontal location is:

$$x_{balistic} = \dot{x}t = \dot{x}\sqrt{\frac{2z_0}{g}} \tag{3-2}$$

which is then compares to the capture point as:

$$x_{balistic} = \sqrt{2}x_{cp} \tag{3-3}$$

This can also be reasoned from a leg force perspective, as no energy is substracted from the CoM during its travel.
Using this formulation of the problem and E_{LIP}:

$$x^2_{balistic} = \frac{z_0}{g}(\dot{x}_0^2 + \dot{x}_f^2) \tag{3-4}$$

Capture limits: leg can apply an infinite force just after the current position to stop on that horizontal location. The other side of the bound is the balistic touch down point, where the virtual leg can apply an impact when the mass hits the ground equal to its velocity and in the direction, then lift the mass up to the desired or default height. This limit on the capture region is defined as:

$$\{x_{cp} \in (0, \dot{x}\sqrt{\frac{2z_0}{g}}]\} \tag{3-5}$$

[1]

3-2 Height Constrained Capture

No leg length constriant, but height constraint.

$$x_{cp,height} = (\frac{\sqrt{2g\delta z_{max}}}{g} + \sqrt{\frac{z_o + \delta z_{max}}{g}})(\dot{x}_0 - \frac{x_0}{z_0}\sqrt{2g\delta z_{max}}). \tag{3-6}$$

3-3 Impact Influenced Capture

$$x_{cp,impact} = \sqrt{\frac{z}{g}}(\dot{x} + \dot{x}_I) \tag{3-7}$$

$$x_{cp,impact} = \sqrt{\frac{z}{g}}(\dot{x} + \frac{x}{z}\dot{z}) \tag{3-8}$$

$$x_{cp,impact} = \frac{z}{\sqrt{zg} - \dot{z}} \tag{3-9}$$

[3], mention also straight leg walking, planning.

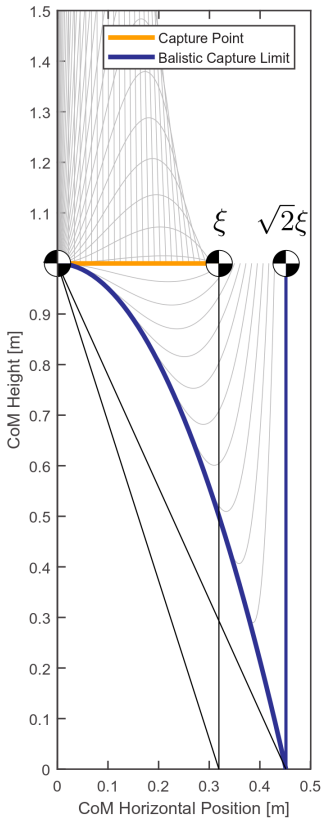
Capture Point
Balistic Capture Limit
ξ
$\sqrt{2}\xi$
CoM Height [m]
CoM Horizontal Position [m]
0
0.1
0.2
0.3
0.4
0.5
0.6
0.7
0.8
0.9
1
1.1
1.2
1.3
1.4
1.5

Figure 3-1

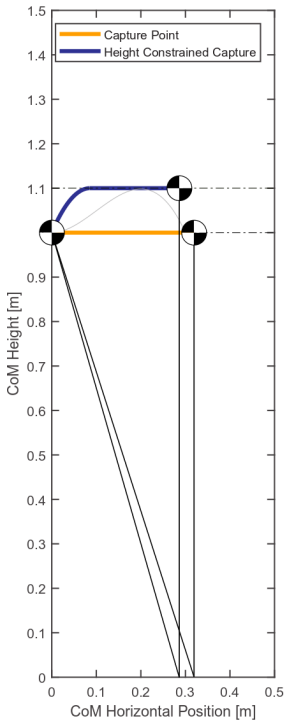
Capture Point
Height Constrained Capture
CoM Height [m]
CoM Horizontal Position [m]
0
0.1
0.2
0.3
0.4
0.5
0.6
0.7
0.8
0.9
1
1.1
1.2
1.3
1.4
1.5

Figure 3-2

Chapter 4

Orbital Energy MPC

4-1 2D Polynomial

$$\frac{1}{2}\dot{x}^2\bar{f}^2(x) + gx^2 f(x) - 3g\int_{x_0}^{x} f(\xi)\xi d\xi = \frac{1}{2}\dot{x}_0^2\bar{f}^2(x_0) + gx_0^2 f(x_0). \tag{4-1}$$

$$u = \frac{g + f''(x)\dot{x}^2}{\bar{f}(x)} \tag{4-2}$$

$$\underbrace{\begin{bmatrix} 1 & 0 & 0 & 0 \\ 1 & x_0 & x_0^2 & x_0^3 \\ 0 & 1 & 2x_0 & 3x_0^2 \\ \frac{3}{2}gx_0^2 & gx_0^3 & \frac{3}{4}gx_0^4 & \frac{3}{5}gx_0^5 \end{bmatrix}}_{A} \underbrace{\begin{bmatrix} c_0 \\ c_1 \\ c_2 \\ c_3 \end{bmatrix}}_{\boldsymbol{c}} = \underbrace{\begin{bmatrix} z_f \\ z_0 \\ \frac{\dot{z}_0}{\dot{x}_0} \\ k \end{bmatrix}}_{\boldsymbol{b}} \tag{4-3}$$

where $k = \frac{1}{2}(\dot{x}_0 z_0 - \dot{x}_0 x_0)^2 + gx_0^2 z_0 - \frac{1}{2}z_f^2\dot{x}_f^2$.

4-1-1 Height Constraint

4-1-2 Leg Length Constraint

4-2 Challenges 3D Orbital Energy

4-3 Results

4-4 Discussion

Algorithm 1 Find cubic polynomial constants under height constraint

procedure FINDPOLZ($A^{-1}, \boldsymbol{b}(\dot{x}_f)$)
  $\dot{x}_f \leftarrow 0$ ▷ Initial guess
  repeat
    $\boldsymbol{c} \leftarrow A^{-1}\boldsymbol{b}(\dot{x}_f)$ ▷ Find polynomial constants
    $x_{zmax} \leftarrow max(\frac{-2c_2 \pm \sqrt{4c_2^2 - 12c_3c_1}}{6c_3})$ ▷ Traj. peak lies on highest x
    $z_{max} \leftarrow c_0 + c_1x_{zmax}^2 + c_2x_{zmax}^3 + c_3x_{zmax}^3$ ▷ Corresponding height
    $\dot{x}_f \leftarrow \dot{x}_f + \alpha$ ▷ Some smart increment
  until $z_{max} < z_{const}$
return $\boldsymbol{c}$
end procedure

Algorithm 2 Find cubic polynomial constants under leg length constraint

procedure FINDPOLL($A^{-1}, \boldsymbol{b}(\dot{x}_f)$)
  $\dot{x}_f \leftarrow 0$ ▷ Initial guess
  repeat
    $\boldsymbol{c} \leftarrow A^{-1}\boldsymbol{b}(\dot{x}_f)$ ▷ Find polynomial constants
    $x_{l^2max,1} \leftarrow \frac{-4c_2^2 + \sqrt{16c_2^4 - 24c_3^2(2+2c_1^2)}}{12c_3^2}$ ▷ $d(f(x)^2 + x^2)/dx = 0$
    $x_{l^2max,2} \leftarrow \frac{-4c_2^2 - \sqrt{16c_2^4 - 24c_3^2(2+2c_1^2)}}{12c_3^2}$ ▷ Complex solutions
    $x_{lmax} \leftarrow -|\sqrt{max(x_{l^2max,1}, x_{l^2max,2)}}|$
    $l_{max}^2 \leftarrow x_{lmax}^2 + (c_0 + c_1x_{zmax}^2 + c_2x_{zmax}^3 + c_3x_{zmax}^3)^2$
    $\dot{x}_f \leftarrow \dot{x}_f + \alpha$ ▷ Some smart increment
  until $l_{max}^2 < l_{const}^2$
return $\boldsymbol{c}$
end procedure

Chapter 5

Towards Application

5-1 Challenges

5-1-1 Angular Momentum and Height Variation

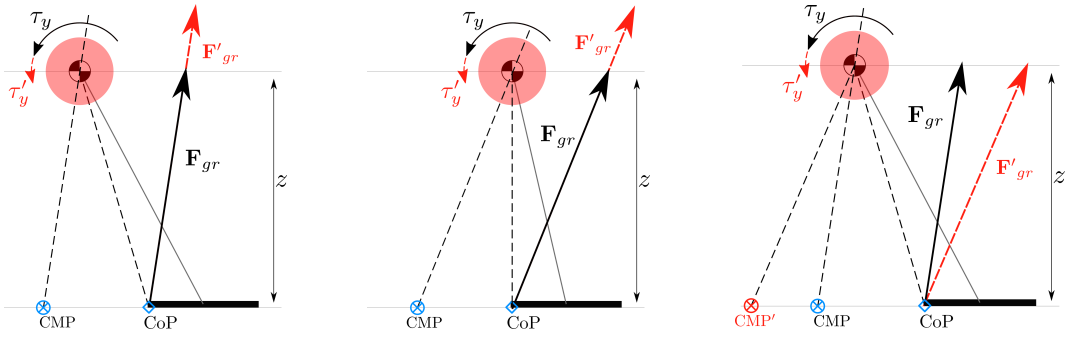

Figure 5-1

5-1-2 From 2D to 3D

Gram determinant. Growth unstable eigenvalue. Coupling xy. 1 input for directions.

5-1-3 Predictability of Dynamics

Wether or not to recover, given foot holds, force limits, height limits, friction limits.

5-1-4 Singularity Avoidance

Stance leg and swing leg.

5-2 Methods

Best you can do. No MPC. Considering footholds are given. Speeding up trajectory?

5-2-1 Adjust Quadratic Program Structure

5-2-2 Adjust Quadratic Program Inputs

Harsh touchdown. Singularity of stance and swing leg. Different strategies.

$$\dot{\mathbf{l}}_d = \frac{\mathbf{c}_{xy} - \mathbf{r}_{cmp,d}}{z} F_z \tag{5-1}$$

$$\dot{\mathbf{l}}_d = \frac{\mathbf{c}_{xy} - (\mathbf{r}_{cop,d} + \frac{\tau_y}{F_z})}{z} F_z \tag{5-2}$$

$$\dot{\mathbf{l}}_d = \frac{\mathbf{c}_{xy} - \mathbf{r}_{cop,d}}{z} m(g + \ddot{z}_d) - \frac{\tau_y}{z} \tag{5-3}$$

$$\dot{\mathbf{l}}_d = \underbrace{\frac{\mathbf{c}_{xy} - \mathbf{r}_{cmp,d}}{z} mg}_{\dot{\mathbf{l}}_{d,lip}} + \underbrace{\frac{\mathbf{c}_{xy} - \mathbf{r}_{cop,d}}{z} m\ddot{z}_d}_{\dot{\mathbf{l}}_{d,heightcontrol}} \tag{5-4}$$

5-3 Experimental Setup

Terrain with limited foot placement options. Push recovery

5-4 Results

5-4-1 Simulation

Comparison with 'normal' control setup. (Comparison with cop / angular momentum?)

5-4-2 Hardware

5-5 Discussion

Chapter 6

Conclusion

6-1 Recommendations

Bibliography

[1] T. Koolen, M. Posa, and R. Tedrake, "Balance control using center of mass height variation: limitations imposed by unilateral contact," in *Humanoid Robots (Humanoids), 2016 IEEE-RAS 16th International Conference on*, pp. 8–15, IEEE, 2016.

[2] S. Kajita, F. Kanehiro, K. Kaneko, K. Yokoi, and H. Hirukawa, "The 3d linear inverted pendulum mode: A simple modeling for a biped walking pattern generation," in *Intelligent Robots and Systems, 2001. Proceedings. 2001 IEEE/RSJ International Conference on*, vol. 1, pp. 239–246, IEEE, 2001.

[3] A. D. Kuo, J. M. Donelan, and A. Ruina, "Energetic consequences of walking like an inverted pendulum: step-to-step transitions," *Exercise and sport sciences reviews*, vol. 33, no. 2, pp. 88–97, 2005.

[4] M. Vukobratović and B. Borovac, "Zero-moment point—thirty five years of its life," *International journal of humanoid robotics*, vol. 1, no. 01, pp. 157–173, 2004.

[5] P. Sardain and G. Bessonnet, "Forces acting on a biped robot. center of pressure-zero moment point," *IEEE Transactions on Systems, Man, and Cybernetics-Part A: Systems and Humans*, vol. 34, no. 5, pp. 630–637, 2004.

[6] M. Vukobratovic and D. Juricic, "Contribution to the synthesis of biped gait," *IEEE Transactions on Biomedical Engineering*, no. 1, pp. 1–6, 1969.

[7] M. B. Popovic, A. Goswami, and H. Herr, "Ground reference points in legged locomotion: Definitions, biological trajectories and control implications," *The International Journal of Robotics Research*, vol. 24, no. 12, pp. 1013–1032, 2005.

[8] S. Kajita, T. Yamaura, and A. Kobayashi, "Dynamic walking control of a biped robot along a potential energy conserving orbit," *IEEE Transactions on robotics and automation*, vol. 8, no. 4, pp. 431–438, 1992.

[9] J. Pratt, J. Carff, S. Drakunov, and A. Goswami, "Capture point: A step toward humanoid push recovery," in *Humanoid Robots, 2006 6th IEEE-RAS International Conference on*, pp. 200–207, IEEE, 2006.

[10] T. Koolen, T. De Boer, J. Rebula, A. Goswami, and J. Pratt, "Capturability-based analysis and control of legged locomotion, part 1: Theory and application to three simple gait models," *The International Journal of Robotics Research*, vol. 31, no. 9, pp. 1094–1113, 2012.

[11] J. E. Pratt and S. V. Drakunov, "Derivation and application of a conserved orbital energy for the inverted pendulum bipedal walking model," in *Robotics and Automation, 2007 IEEE International Conference on*, pp. 4653–4660, IEEE, 2007.

[12] L. Lanari, S. Hutchinson, and L. Marchionni, "Boundedness issues in planning of locomotion trajectories for biped robots," in *Humanoid Robots (Humanoids), 2014 14th IEEE-RAS International Conference on*, pp. 951–958, IEEE, 2014.

[13] J. Englsberger, C. Ott, and A. Albu-Schäffer, "Three-dimensional bipedal walking control using divergent component of motion," in *Intelligent Robots and Systems (IROS), 2013 IEEE/RSJ International Conference on*, pp. 2600–2607, IEEE, 2013.

[14] M. A. Hopkins, D. W. Hong, and A. Leonessa, "Humanoid locomotion on uneven terrain using the time-varying divergent component of motion," in *Humanoid Robots (Humanoids), 2014 14th IEEE-RAS International Conference on*, pp. 266–272, IEEE, 2014.

[15] C. R. Lee and C. T. Farley, "Determinants of the center of mass trajectory in human walking and running.," *Journal of experimental biology*, vol. 201, no. 21, pp. 2935–2944, 1998.

[16] W. Gao, Z. Jia, and C. Fu, "Increase the feasible step region of biped robots through active vertical flexion and extension motions," *Robotica*, vol. 35, no. 7, pp. 1541–1561, 2017.

[17] S. Caron, A. Escande, L. Lanari, and B. Mallein, "Capturability-based analysis, optimization and control of 3d bipedal walking," *arXiv preprint arXiv:1801.07022*, 2018.

Glossary

List of Acronyms

ICP	instantaneous capture point
CP	capture point
ZMP	zero moment point
CoP	center of pressure
CoM	center of mass
CMP	centroidal momentum pivot
LIP	linear inverted pendulum
2D	two-dimensional space
3D	three-dimensional space
GRF	ground reaction force

List of Symbols

E_{LIP}	LIP orbital energy
E_{orbit}	Nonlinear orbital energy